Received: 8 May 2023 | Accepted: 18 March 2024

DOI: 10.1002/pros.24701

ORIGINAL ARTICLE

The Prostate WILEY

An orthotopic prostate cancer model for new treatment development using syngeneic or patient-derived tumors

Naz Chaudary PhD[1] | E. Wiljer BSc[1] | Warren Foltz PhD[1] | Pratibha Thapa MSc[1] | Richard P. Hill PhD[1,2,3] | Michael Milosevic MD[1,2,4]

[1]Princess Margaret Cancer Centre, Toronto, Canada

[2]Department of Radiation Oncology, University of Toronto, Toronto, Canada

[3]Department of Medical Biophysics, University of Toronto, Toronto, Canada

[4]Institute of Medical Science, University of Toronto, Toronto, Canada

Correspondence
Michael Milosevic, MD, University Health Network and Princess Margaret Cancer Centre, 610 University Ave, Toronto, ON M5G 2M9, Canada.
Email: mike.milosevic@uhn.ca

Funding information
This work was supported by grants from the Terry Fox Research Institute (Terry Fox New Frontier Program Project Grants #20005 and #1036) and by the Princess Margaret Cancer Foundation.

Abstract

Background: There are limited preclinical orthotopic prostate cancer models due to the technical complexity of surgical engraftment and tracking the tumor growth in the mouse prostate gland. Orthotopic xenografts recapitulate the tumor microenvironment, tumor stromal interactions, and clinical behavior to a greater extent than xenografts grown at subcutaneous or intramuscular sites.

Methods: This study describes a novel micro-surgical technique for orthotopically implanting intact tumors pieces from cell line derived (transgenic adenocarcinoma mouse prostate [TRAMP]-C2) or patient derived (neuroendocrine prostate cancer [NEPC]) tumors in the mouse prostate gland and monitoring tumor growth using magnetic resonance (MR) imaging.

Results: The TRAMP-C2 tumors grew rapidly to a predetermined endpoint size of 10 mm within 3 weeks, whereas the NEPC tumors grew at a slower rate over 7 weeks. The tumors were readily detected by MR and confidently identified when they were approximately 2–3 mm in size. The tumors were less well-defined on CT. The TRAMP-C2 tumors were characterized by amorphous sheets of poorly differentiated cells similar to a high-grade prostatic adenocarcinoma and frequent macroscopic peritoneal and lymph node metastases. In contrast, the NEPC's displayed a neuroendocrine morphology with polygonal cells arranged in nests and solid sheets and high count. There was a local invasion of the bladder and other adjacent tissues but no identifiable metastases. The TRAMP-C2 tumors were more hypoxic than the NEPC tumors.

Conclusions: This novel preclinical orthotopic prostate cancer mouse model is suitable for either syngeneic or patient derived tumors and will be effective in developing and advancing the current selection of treatments for patients with prostate cancer.

KEYWORDS
orthotopic tumor model, prostate cancer

[†]We dedicate this paper in memory of Dr. Richard P. Hill to acknowledge his contributions. Dr. Hill is recently deceased but was involved in this work and qualifies for authorship.

1 | INTRODUCTION

Prostate cancer is the second most common cancer in men worldwide after lung cancer.[1] In 2020, more than 1.4 million men were diagnosed with prostate cancer, and more than 375,000 men died of the disease.[1]

The human prostate gland consists of three distinct zones: the transitional, central, and peripheral zones. The peripheral zone consists of the posterior and lateral portions of the prostate and contains 70%–80% of the glandular tissue.[2] Most prostate cancers are adenocarcinomas and most commonly occur in the peripheral zone. Metastases arise in pelvic lymph nodes and in the liver, lungs, and bones.[3] Current treatments for prostate cancer include active surveillance, surgery, radiation therapy, androgen deprivation therapy, cytotoxic chemotherapy, and immunotherapy. While the long term survival of men with localized prostate cancer is 70% or higher with currently available treatments, metastatic prostate cancer is incurable.[4] The high mortality is, in part, attributed to a lack of effective treatments that account for the high degree of heterogeneity in the tumor cells and their microenvironment.

1.1 | Preclinical prostate models

Preclinical prostate cancer research has been restricted by a deficit of clinically relevant laboratory models for in vivo study of the molecular and immune mechanisms of prostate tumorigenesis, progression, and treatment response in mice. A common approach has been to use human tumor cell lines or tissues implanted subcutaneously in recipient immunocompromised mice. A variety of tumor models based on immortalized cell lines or preserved and passaged tumor biopsies from patients with prostate cancer have been described.[5–9] A major limitation is the requirement for an immunosuppressed host system, which limits the ability to study the immune microenvironment and immunotherapy. Genetically engineered syngeneic prostate cancer mouse models (GEMMs) driven by specific genetic mutations facilitate the use of fully immunocompetent mice and overcome this limitation. One of the most widely studied syngeneic prostate cancer models is the transgenic adenocarcinoma mouse prostate (TRAMP) model, which utilizes the prostate-specific probasin promoter to express the SV40 T-antigen (Tag) viral oncogene.[10–13] TRAMP mice develop epithelial hyperplasia at 8 weeks of age, prostate intraepithelial neoplasia at 18 weeks, and lymph node and distant metastasis at 28 weeks. TRAMP tumors are hormonally independent, similar to castrate-resistant prostate cancer in humans.

Subcutaneous xenograft mouse models are commonly used as they are simple to generate and monitor. However, orthotopic xenografts may better recapitulate the tumor microenvironment, tumor stromal interactions, and clinical behavior of human tumors.[14–16] Compared to subcutaneous or intramuscular tumors, orthotopic xenograft mouse models allow implanted tumors to develop and progress in a local milieu that more closely mirrors patients and have been advocated as preferred models for studying new combinations of radiotherapy or cytotoxic chemotherapy with molecular targeted treatments.

1.2 | Aim of study

Despite the potential advantages, very few orthotopic prostate cancer models have been described previously,[17,18] in part because of the complexity of implanting and monitoring tumor growth in the mouse prostate gland. We previously described a method for establishing patient derived, orthotopic cervical cancer xenografts for studying radiation sensitizers.[19–23] Here, we extend our previous work and describe a novel technique for establishing an orthotopic prostate cancer mouse model suitable for either patient-derived or syngeneic tumors and monitoring tumor progression over time or in response to treatment using magnetic resonance (MR) imaging. We describe the orthotopic implantation technique using intact tumor pieces derived from cell lines or patient biopsies and illustrate the advantages of MR compared to CT imaging. This novel technique provides a framework in which to study tumor cell interactions with the prostatic microenvironment and treatment response throughout disease evolution. Orthotopic implantation of tumor pieces facilitates the preservation of tumor cell heterogeneity for the study of cellular and molecular interactions among different cell types and may be more representative of the biology in real patients in the clinic.

2 | MATERIALS AND METHODS

2.1 | Tumor and mouse models

Two prostate tumor models were used to illustrate the orthotopic implantation technique. The first was derived from the TRAMP-C2 cell line. TRAMP-C2 donor tumors for orthotopic implantation were established by injecting 3×10^6 TRAMP-C2 cells (provided by S. Liu; Sunnybrook Research Institute) subcutaneously in the flanks of 6–8 week old C57BL/6 (Jackson Laboratory) male mice. TRAMP-C2 tumors are hormonally independent, similar to castrate-resistant prostate cancer in humans.[12]

The second tumor model was a patient-derived neuroendocrine prostate cancer (NEPC) provided by H. He, Princess Margaret Research Institute and Y. Z. Wang, Vancouver Prostate Centre. The LTL-545 NEPC model [8,24] was derived in 2013 from the primary tumor of a patient with treatment-naïve, poorly differentiated NEPC. The model was originally established at the subrenal site in NOD/SCID mice and cryopreserved for future grafting. It was previously characterized as being androgen independent with histopathologic features of NEPC, including small cell morphology, negative staining for androgen receptor and PSA, and high expression of the neuroendocrine markers chromogranin A and synaptophysin.[8,24] NEPC donor tumors for this study were established by implanting tumor pieces 2–3 mm in size subcutaneously in the flanks of 6–8 week old NOD SCID male mice (Princess Margaret Research Institute breeding colony).

The mouse prostate gland, in contrast to the human, consists of four paired lobes: the anterior, dorsal, ventral, and lateral lobes[25,26] (Figure 1H). The dorsal, ventral, and lateral lobes are located around the urethra below the bladder. The anterior lobes are located cranial to the other lobes in proximity to the seminal vesicles. In mice, the

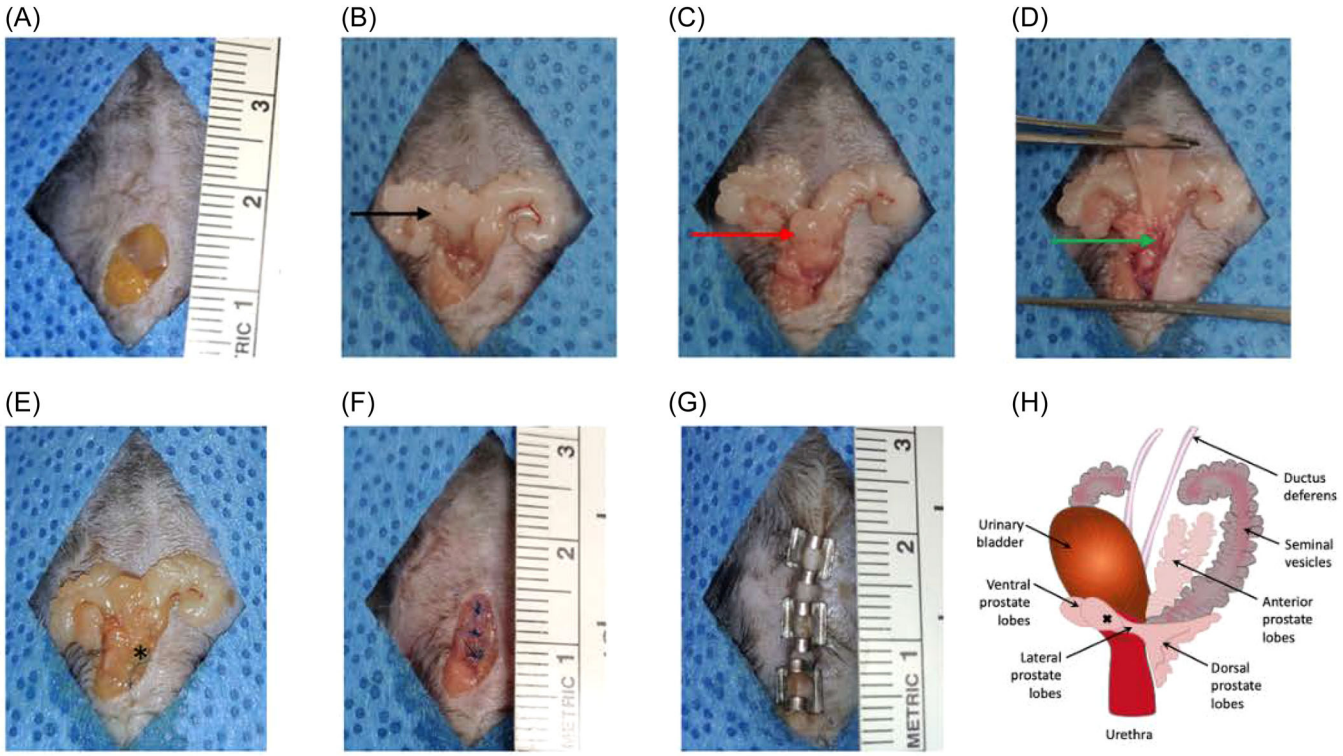

FIGURE 1 Surgical technique for implanting tumor pieces derived from cell lines or patient biopsies into the prostate glands of male mice. (A) 1–2 cm mid-line incision is made in the skin of the lower abdomen and the adhesions between the skin and peritoneal membrane are loosened. (B) A smaller incision is made in the peritoneum. The seminal vesicles (black arrow) are externalized using forceps. (C) The bladder (red arrow) is externalized using forceps. (D) Holding the bladder with forceps, a small 1 mm incision is made in the ventral prostate lobe under the bladder (green arrow). (E) The suture with the tumor fragment threaded onto it is passed from the inside to the outside of the ventral prostate at the incision site and the fragment is sutured onto the prostate lobe (* indicates the sutured tumor fragment). (F) The tissues are returned to the peritoneal cavity. The peritoneum is closed with 2–3 sutures. (G) The skin is closed with 3–4 wound clips. The incision is sterilized with ethanol. (H) A schematic illustration of the anatomy of the mouse prostate, adapted from Ittmann et al.[26] X indicates site of tumor implantation in the prostate gland. [Color figure can be viewed at wileyonlinelibrary.com]

dorsolateral prostate lobes are homologous to the peripheral zones of the human prostate.[27] Once established, TRAMP-C2 donor tumors were excised and transplanted to the dorsolateral prostate lobes of C57BL/6 male mice; NEPC donor tumors were transplanted to the dorsolateral prostate lobes of immunosuppressed NOD-Rag1^{null}IL2rg^{null} (NRG, Jackson Laboratories, Princess Margaret Research Institute breeding colony) male mice. All experiments were performed according to protocols approved under the regulations of the Canadian Council on Animal Care and Use.

2.2 | Surgical supplies for orthotopic transplantation

1. Alpha-Minimal Essential Medium (alpha-MEM) containing penicillin and streptomycin antibiotics and FBS,
2. Betadine and surgical scrub,
3. Nose-cone anesthetic machine,
4. Isoflurane for inhalation anesthesia,
5. Meloxicam 0.5 mg/mL solution in saline,
6. Syringes 1.0 mL with 27 G needles,
7. Eye gel (tear-gel; Novartis),
8. Disposable scalpel blades #11,
9. Electric shaving razor,
10. Heating pad,
11. Sterile gauze pads,
12. Sterile swabs,
13. Scissors (fine surgical),
14. Forceps (fine),
15. Scalpel and disposable blades,
16. Small hemostat and needle driver,
17. Wound clips 9 mm with applier and remover,
18. 6-0 proline monofilament suture nonabsorbable,
19. 70% (v/v) ethanol solution in demineralized water.

2.3 | Surgical technique for orthotopic transplantation

1. The day of implantation, anesthetize the mice bearing the donor tumors using 2% isoflurane inhalation and then euthanize by cervical dislocation.

2. Rapidly excise the donor tumor in a biosafety cabinet using scissors and forceps.
3. Place the donor tumor on a 60 mm^2 cell culture dish containing sterile ice-cold complete alpha-MEM.
4. Using forceps and a scalpel, slice the tumor into small cubic fragments of 2–3 mm^3. Place the tumor fragments in alpha-MEM on ice. Select tumor fragments that are solid, uniform in color, homogenous, and lacking any necrosis and blood clots for orthotopic implantation.
5. Thread the selected tumor fragment onto the suture material and return it to alpha-MEM on ice. The suture should pass through the center of the tumor piece.
6. Anesthetize the recipient mouse using isoflurane inhalation and a nose cone with a 5% induction phase, followed by 2% maintenance phase. Following placement of the nose cone, apply eye gel.
7. Inject 0.1 mL meloxicam analgesic subcutaneously. Administer 0.1 mL of saline subcutaneously to keep the animal hydrated throughout the procedure. Place a heating pad under the sterile bench pad to keep the animal warm.
8. Remove the hair on the lower abdomen at the surgical site using an electric razor.
9. Sterilize the lower abdomen with iodine scrub solution followed by an antiseptic betadine skin surgical scrub, and clean with 70% ethanol. Pat dry.
10. Lift the skin away from the lower abdomen using forceps and make a horizontal 1.5–2.0 cm midline incision with a sterile scalpel above the preputial gland. Use a hemostat to loosen the adhesion between the skin and peritoneal membrane (Figure 1A). This will facilitate easy suturing of the peritoneal incision when closing.
11. Once the abdominal wall is exposed, make a smaller 1.0 cm midline incision in the peritoneum.
12. Using blunt-ended forceps, push aside the fat and externalize the bladder. The bladder may also be located by first externalizing the seminal vesicles (Figure 1B). Directly above the preputial glands, insert the forceps laterally into the peritoneal cavity at a 45° angle from the incision to externalize the seminal vesicles. The seminal vesicles are delicate and should be pulled up from the base rather than the ends, being careful not to tear the tissue. Pulling the seminal vesicles up will help externalize the bladder (taking care not to puncture the bladder) (Figure 1C).
13. Gently place forceps under the bladder to prevent it from sliding back into the peritoneal cavity. Locate the ventral prostate lobes under the bladder and next to the seminal vesicles. The lobes are soft so care must be taken not to tear the tissue. Holding the base of the bladder gently with forceps, make a small 1 mm incision along the ventral prostate lobe (Figure 1D).
14. Pass the suture with the tumor fragment (without matrigel) from the inside to the outside of the prostate at the incision point and knot the tumor fragment so that it is in direct contact with the ventral prostate. Place additional sutures to secure the fragment (Figure 1E).
15. Return the bladder and seminal vesicles to their original locations in the peritoneal cavity.
16. Close the peritoneum with 2–3 sutures (Figure 1F).
17. Using forceps, pinch the edges of the skin together along the length of the incision and close the skin with 3–4 wound clips (Figure 1G).
18. Sterilize the sealed skin incision with 70% ethanol.

2.4 | Postoperative care

1. Following closure of the surgical site, place the animal on a heating pad to maintain normal body temperature during recovery from anesthesia.
2. Place the animal in a clean cage supplied with food and water containing the antibiotic Clavamox (0.5 mg/mL), additional nutritional supplements (Ensure/KMR) for 48 h after surgery.
3. Monitor mice for up to 2 h after surgery until they are active.
4. Monitor mice daily for signs of illness or infection, including reduced or slowed movement, weakness, hunched posture, weight loss, lack of grooming, or difficulty breathing.
5. Remove the wound clips 7–10 days postimplantation using a wound clip remover.

2.5 | MR and CT imaging of tumor growth and treatment response

MR and CT imaging was initiated 12 days after tumor implantation, the earliest time that growing tumors could reliably be identified, and was performed approximately weekly thereafter.

MR images were acquired using a preclinical 7T MRI (Biospec 70/30 USR; Bruker) equipped with the B-GA12 gradient coil insert and 72 mm inner diameter cylindrical transmit/receive quadrature volume coil. Mice were immobilized in the prone position on a vendor-supplied bed and anesthetized with 1.8% isoflurane through a nose cone. Axial 2D T2-weighted rapid acquisition with relaxation enhancement (RARE) images were acquired for each mouse, encompassing the prostate region (effective echo time 40 ms; echo time 8 ms; RARE factor 10; repetition time 4000 ms; 128 × 128 matrix over 32 × 32 mm field-of-view for 250 μ in-plane resolution; at least 25 slices; 1 mm slice thickness; 3 averages). The acquisition time was 5 min. Cone-beam CT (CBCT) imaging for radiation treatment planning was done using a small animal imager and irradiator (X-Rad 225Cx, Precision X-ray) with 40 KVp, 5–7 mA at 0.2 mm voxel resolution. Prostate tumor volume at each timepoint was calculated by first contouring the tumor on each axial MR slice in which it was visible (approximately 5–10 slices depending on tumor size and regularity of shape) using the Inveon Research Workplace, IRW 4.0 preclinical software (Siemens Medical Solutions USA Inc.). The tumor volume represented by each contoured region was determined from the number and size (0.0625 mm^2) of the contained pixels multiplied by the MR slice thickness (1 mm). The axial volumes were then

summed to obtain the overall tumor volume. Tumors were not contoured on CBCT because they could not be seen clearly. All imaging was performed at the UHN STTARR Innovation Core Facility.

Tumors were contoured separately by two independent observers. The tumor volumes from the two observers were compared using a linear mixed effects statistical model. Volume was log transformed to stabilize the variance of the residuals. Time was considered a fixed effect, as it was expected that tumor growth would occur over time.

Tumor hypoxia was measured by injecting the hypoxia marker drug EF5 (2-(2-Nitro-1H-imidazole-1-yl)-N-(2,2,3,3,3-pentafluoropropyl) acetamide) 10 mg/kg intravenously 3 h before euthanizing the mice. Immunohistochemistry (IHC) was used to visualize EF5 staining. Hypoxic fraction was calculated as the number of strongly staining pixels per image divided by the total number of pixels. Synaptophysin and Ki67 were also evaluated by IHC in a representative NEPC tumor.

3 | RESULTS

There was 100% success rate in establishing the TRAMP-C2 and NEPC orthotopic tumors. Serial MR imaging every 1–2 weeks was used to monitor tumor growth. Figure 2 shows representative axial, T2-weighted MR, and CBCT images of a TRAMP-C2 tumor and NEPC in the mouse prostate 1 week after implantation. The tumors were readily detected by MR (Figure 2A,B) and confidently identified when they were approximately 2–3 mm in size. The tumors were less well-defined on CBCT (Figure 2C,D). The TRAMP-C2 tumors grew rapidly to a predetermined endpoint size of 10 mm within 3 weeks, whereas the NEPC tumors grew at a slower rate over 7 weeks (Figure 3).

Two independent observers contoured the tumors on each axial MR image slice to estimate tumor volume. The tumor volumes from the two observers were compared using a mixed effects statistical model. Of the total sample variance, 86% was attributable to "true" differences in tumor volume agreed upon by the two observers, while 14% was due to differences between the observers. This suggests that MR imaging of orthotopic mouse prostate tumors, as performed in this study, provides a reliable measure of tumor volume over time.

The mice were euthanized when the primary tumors reached the endpoint size. The primary tumors, any enlarged lymph nodes, lungs, liver, kidneys, and intestine, were excised for histologic assessment by a veterinary pathologist. The TRAMP-C2 tumors were characterized by amorphous sheets of poorly differentiated cells similar to a high-grade prostatic adenocarcinoma (Figure 4A) and frequent macroscopic peritoneal and lymph node metastases. In contrast, the NEPC's displayed a neuroendocrine morphology with polygonal cells arranged in nests and solid sheets, small to moderate amounts of vacuolated eosinophilic cytoplasm, only small amounts of fibrous stroma, and a mitotic count of 30–50 per 10 40× field (Figure 4B). There was a local invasion of the bladder and other adjacent tissues but no identifiable metastases. Both the TRAMP-C2 and NEPC tumors were comprised of greater than 70% tumors cells, with the stromal components representing less than 30%. The mean (±standard error) hypoxic fraction measured by EF5 staining was higher in TRAMP-C2 (39 ± 0.9%) than in NEPC (13 ± 2.0%), as highlighted in Figure 4C,D.

The NEPC tumors were stained positively for synaptophysin by IHC (Figure 4E), a marker of neuroendocrine differentiation, and the proliferation marker Ki67 (Figure 4F). Negative synaptophysin staining in a control, patient dervied cervical cancer xenograft (Figure 4G).

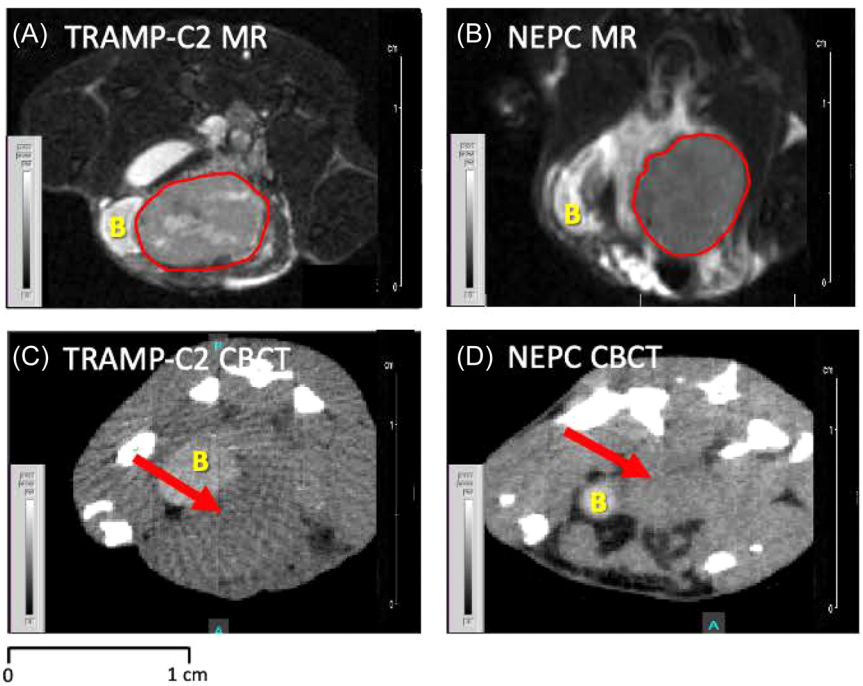

FIGURE 2 Representative axial, T2-weighted MR (A, B), and CBCT (C, D) images of 8–9 mm TRAMP-C2 and NEPC orthotopic prostate xenografts (red contours and arrows) 3–4 weeks after implantation. The prostate tumors were more clearly seen and could be more confidently delineated on MR than on CT. As the tumors grew, they infiltrated the entire prostate gland making it difficult to identify the prostate or seminal vesicle anatomy in greater detail. The urinary bladder (B) is also identified. The mice were positioned prone for imaging. CBCT, cone-beam CT; MR, magnetic resonance; NEPC, neuroendocrine prostate cancer; TRAMP, transgenic adenocarcinoma mouse prostate. [Color figure can be viewed at wileyonlinelibrary.com]

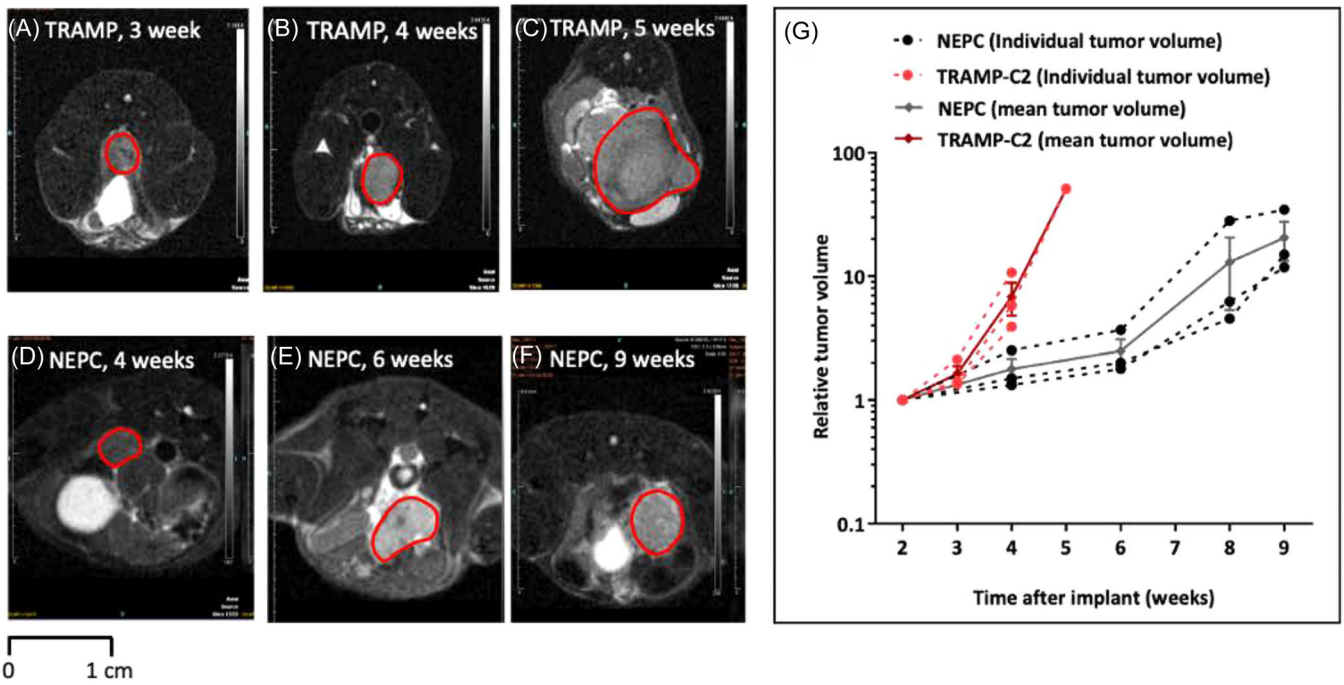

FIGURE 3 Representative axial, T2-weighted MR images illustrating the growth of orthotopic TRAMP-C2 (A–C) and NEPC (D–F) prostate cancer xenografts at three time points after implantation. The prostate tumors are delineated in red at each timepoint. The TRAMP-C2 tumors grew faster than the NEPC tumors. Also shown is relative tumor volume for the two models (G) as a function of time after implantation. Relative tumor volume was calculated by normalizing future volumes to the volume on Day 12 following implantation, the earliest time that growing tumors could reliably be identified. Relative volumes of the individual tumors are shown as dotted lines, and the mean (±SEM) relative volumes as solid lines. There were three mice per group. The mice were positioned prone for imaging. MR, magnetic resonance; NEPC, neuroendocrine prostate cancer; TRAMP, transgenic adenocarcinoma mouse prostate. [Color figure can be viewed at wileyonlinelibrary.com]

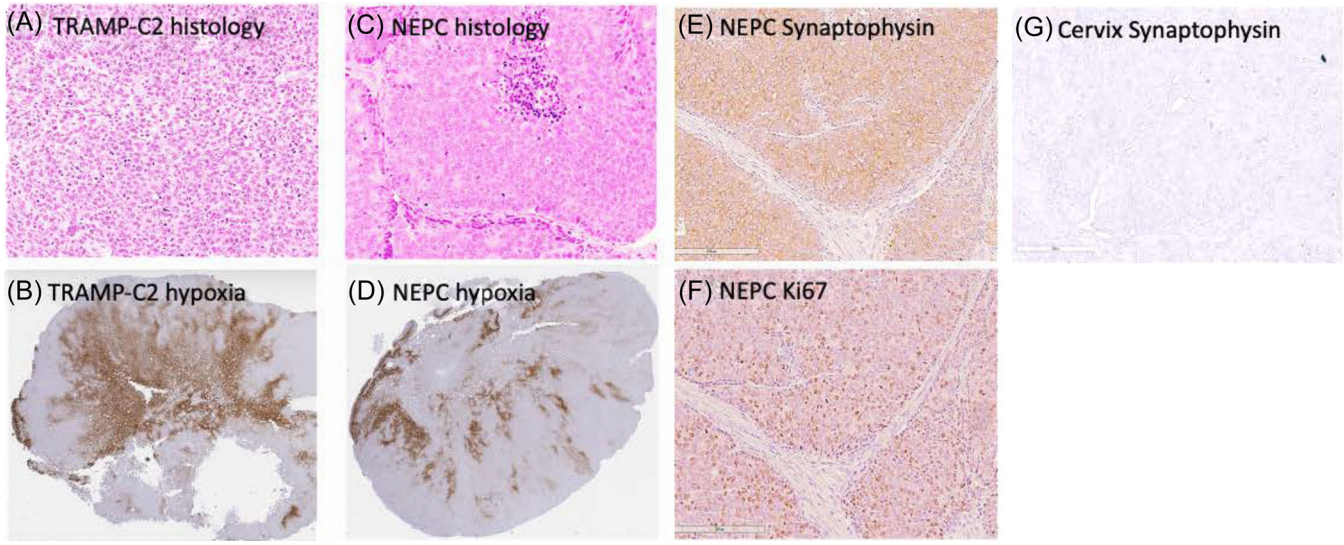

FIGURE 4 Representative hematoxylin and eosin images (×20 magnification) (A, C) and EF5-stained images (×10 magnification) of tumor hypoxia (B, D) in TRAMP-C2 and NEPC tumors. The mean (±standard error) hypoxic fraction was higher in TRAMP-C2 (39 ± 0.9%) than in NEPC (13 ± 2.0%). Also shown are representative images of positive synaptophysin (E) and Ki67 (F) staining in the NEPC tumor and negative synaptophysin staining in a control, patient derived cervical cancer xenograft (G). EF5, (2-(2-nitro-1H-imidazole-1-yl)-N-(2,2,3,3,3 pentafluoropropyl)acetamide); NEPC, neuroendocrine prostate cancer; TRAMP, transgenic adenocarcinoma mouse prostate. [Color figure can be viewed at wileyonlinelibrary.com]

4 | DISCUSSION

Most patients with prostate cancer are diagnosed with low or intermediate risk disease that is confined to the prostate gland. However, the disease may evolve over time or in response to treatment to a more locally aggressive or metastatic phenotype. New treatments are needed at every stage of this evolution. However, prostate cancer research has been limited by a lack of relevant preclinical models that mirror the clinical setting. The common prostate cancer models use immortalized cell lines or preserved and passaged tumor biopsies from patients with prostate cancer growing subcutaneously in immune deficient mice.[5–9] These subcutaneous tumors may be less representative of human cancer, in part because of the ectopic host tumor microenvironment.[14–16]

This study describes a novel technique for establishing an orthotopic prostate cancer mouse model suitable for either syngeneic or patient-derived tumors and monitoring tumor progression over time or in response to treatment using MR imaging. The mouse prostate gland differs from the human in that it has four paired lobes without a fibrous capsule and is located in the abdomen.[28] Our technique involves micro-surgical implantation of tumor pieces directly onto the dorsolateral prostate lobe. Lardizabal et al. generated orthotopic TRAMP-C2 tumors by injecting cells into the prostate gland under direct ultrasound guidance.[17] However, to our knowledge, only one previous study [18] described direct orthotopic implantation of prostate tumor pieces onto the prostate gland, which may be more biologically and clinically relevant than cell injection by better preserving tumor heterogeneity and the de novo tumor microenvironment. As well, the technique facilitates the use of tumor models that are not cell-line based, including patient-derived xenografts.

The TRAMP-C2 and patient-derived NEPC orthotopic models described here have different strengths and limitations, as summarized in Table 1. The TRAMP-C2 orthotopic model may be most suitable for immune or metastasis studies when rapid tumor growth is an advantage and the limitations of an immortalized cell line tumor are less important. In contrast, the patient derived NEPC model may be more representative of the genetic and molecular state of high-grade human prostate cancer but requires a host with impaired adaptive immunity. Of note, our orthotopic implantation and MR monitoring approach potentially is applicable to a wide range of prostate cell line, PDX, or syngeneic tumors,[5–9,12] the choice of which will depend on the specific molecular, genetic, or microenvironmental features of greatest interest in a particular study.

The size of subcutaneous xenografts can be measured easily using calipers. However, orthotopic prostate tumors are inaccessible for caliper measurements [28] and more advanced imaging-based techniques are required to track tumor size over time. High resolution ultrasound and bioluminescence imaging of luciferase expressing tumor cells[17] have been described previously. In our study, we have shown the ease of detecting and measuring the size of orthotopic mouse prostate tumors using T2-weighted MR without the need for contrast in vivo. MR region of interest contours on serial axial tumor slices were used to reliably generate quantizable tumor volumes as small as 5 mm^3 (2–3 mm linear dimension) for image analysis. The tumors were readily detected by MR and confidently identified when they were approximately 2–3 mm in size. We found minimal interobserver variability in MR-based tumor volume measurement, with 86% of the total sample variance attributable to true differences in volume (14% attributable to interobserver variability). Tumors smaller than 5 mm^3 had heterogenous contrast and unclear borders between the tumor and surrounding normal tissues.

TABLE 1 Advantages and disadvantages of TRAMP-C2 and NEPC orthotopic prostate xenografts used in this study.

	TRAMP-C2	NEPC
Advantages	• Genetically engineered, syngeneic model • Rapid growth (weeks) • Well characterized • Suitable for immune studies • Suitable for metastasis studies	• Patient derived prostate cancer model • Genetically representative of high-grade human prostate cancer • Suitable for genetic and molecular studies of radiosensitizers and other treatments
Disadvantages	• Immortalized, cell line mouse model • Genetically less representative of human prostate cancer • Radioresistant	• Slower growth (months) • Requires host with impaired adaptive immunity • Not suitable for immune studies

Abbreviations: NEPC, neuroendocrine prostate cancer; TRAMP, transgenic adenocarcinoma mouse prostate.

Hypoxia is present in most solid tumors, including prostate cancer, and is a central driver of genomic instability, malignant progression, metastases, and treatment response.[29,30] In prostate cancer, hypoxia has been reported to influence recurrence after surgery or radiotherapy and progression toward more malignant and metastatic phenotypes, including NEPC.[31–35] In the preclinical setting, tumor hypoxia has been reported to vary depending on the tumor model and implantation site.[15] The two orthotopic models used in this study had different levels of hypoxia that were relatively consistent within each model (TRAMP-C2 39 ± 0.9%, NEPC 13 ± 2.0%). It may be important to include tumor models with different levels of hypoxia when studying prostate cancer progression or new prostate cancer treatments to better approximate real-world conditions in patients.

5 | CONCLUSION

We describe a novel orthotopic prostate cancer mouse model suitable for either syngeneic or patient derived tumors. The main advantage compared to other models is that it accounts for the interaction between tumor cells and the prostatic microenvironment,

which is important in prostate cancer evolution and response to treatments like radiotherapy and immunotherapy. Tumor growth and treatment response can be reliably measured using longitudinal MR imaging. Overall, the model provides a clinically relevant platform for studying new prostate cancer treatments and biomarkers of response with the potential to accelerate translation from the laboratory to the clinic.

ACKNOWLEDGMENTS

The authors thank Dr. Stanley Liu, Dr. Hansen He, and Dr. Y. Z. Wang for providing the tumor models used in this study, Dr. Suzee Camilleri, Dr. Meegan Larsen, and Dr. Joerg Schwock for help with the histological analysis, and Melania Pintilie for help with the statistical analysis. We dedicate this paper in memory of Dr Richard P. Hill for his contributions to preclinical tumor model development over many years. Funding for this work was provided by the Terry Fox Research Institute and The Princess Margaret Cancer Foundation.

CONFLICT OF INTEREST STATEMENT

The authors declare no conflict of interest.

DATA AVAILABILITY STATEMENT

The data that support the findings of this study are available from the corresponding author upon reasonable request.

ORCID

Naz Chaudary http://orcid.org/0000-0002-8021-3182

REFERENCES

1. Sung H, Ferlay J, Siegel RL, et al. Global cancer statistics 2020: GLOBOCAN estimates of incidence and mortality worldwide for 36 cancers in 185 countries. *CA Cancer J Clin*. 2021;71(3):209-249. doi:10.3322/caac.21660
2. Wang G, Zhao D, Spring DJ, DePinho RA. Genetics and biology of prostate cancer. *Genes Dev*. 2018;32(17-18):1105-1140. doi:10.1101/gad.315739.118
3. Valkenburg KC, Williams BO. Mouse models of prostate cancer. *Prostate Cancer*. 2011;2011:1-22. doi:10.1155/2011/895238
4. Klusa D, Lohaus F, Furesi G, et al. Metastatic spread in prostate cancer patients influencing radiotherapy response. *Front Oncol*. 2021;10. doi:10.3389/fonc.2020.627379
5. Cacciatore A, Albino D, Catapano CV, Carbone GM. Preclinical models of neuroendocrine prostate cancer. *Current Protocols*. 2023;3(5):e742. doi:10.1002/cpz1.742
6. Moya L, Walpole C, Rae F, et al. Characterisation of cell lines derived from prostate cancer patients with localised disease. *Prostate Cancer Prostatic Dis*. 2023;26(3):614-624. doi:10.1038/s41391-023-00679-x
7. Shi C, Chen X, Tan D. Development of patient-derived xenograft models of prostate cancer for maintaining tumor heterogeneity. *Transl Androl Urol*. 2019;8(5):519-528. doi:10.21037/tau.2019.08.31
8. Shi M, Wang Y, Lin D, Wang Y. Patient-derived xenograft models of neuroendocrine prostate cancer. *Cancer Lett*. 2022;525:160-169. doi:10.1016/j.canlet.2021.11.004
9. Wu X, Gong S, Roy-Burman P, Lee P, Culig Z. Current mouse and cell models in prostate cancer research. *Endocr Relat Cancer*. 2013;20(4):R155-R170. doi:10.1530/ERC-12-0285
10. Gingrich JR, Barrios RJ, Morton RA, et al. Metastatic prostate cancer in a transgenic mouse. *Cancer Res*. 1996;56(18):4096-4102.
11. Gingrich JR, Greenberg NM. A transgenic mouse prostate cancer model. *Toxicol Pathol*. 1996;24(4):502-504. doi:10.1177/019262339602400414
12. Hurwitz AA, Foster BA, Allison JP, Greenberg NM, Kwon ED. The TRAMP mouse as a model for prostate cancer. *Curr Protocols Immunol*. 2001;45:20.5.1-20.5.23. doi:10.1002/0471142735.im2005s45
13. Kido LA, de Almeida Lamas C, Maróstica Jr. MR, Cagnon VHA. Transgenic adenocarcinoma of the mouse prostate (TRAMP) model: a good alternative to study PCa progression and chemoprevention approaches. *Life Sci*. 2019;217:141-147. doi:10.1016/j.lfs.2018.12.002
14. Gengenbacher N, Singhal M, Augustin HG. Preclinical mouse solid tumour models: status quo, challenges and perspectives. *Nat Rev Cancer*. 2017;17(12):751-765. doi:10.1038/nrc.2017.92
15. Zhang W, Fan W, Rachagani S, et al. Comparative study of subcutaneous and orthotopic mouse models of prostate cancer: vascular perfusion, vasculature density, hypoxic burden and BB2r-targeting efficacy. *Sci Rep*. 2019;9(1):11117. doi:10.1038/s41598-019-47308-z
16. Zheng D. Orthotopic tumours, a hot topic for xenograft models. *EBioMedicine*. 2019;41:11-12. doi:10.1016/j.ebiom.2019.02.052
17. Lardizabal J, Ding J, Delwar Z, Rennie PS, Jia W. A TRAMP-derived orthotopic prostate syngeneic (TOPS) cancer model for investigating anti-tumor treatments. *Prostate*. 2018;78(6):457-468. doi:10.1002/pros.23490
18. Saar M, Körbel C, Linxweiler J, et al. Orthotopic tumorgrafts in nude mice: a new method to study human prostate cancer. *Prostate*. 2015;75(14):1526-1537. doi:10.1002/pros.23027
19. Chaudary N, Hill RP, Stulik L, Milosevic M. The oral CXCR4 inhibitor X4-136 improves tumor control and reduces toxicity in cervical cancer treated with radiation therapy and concurrent chemotherapy. *Int J Radia Oncol*Biol*Phy*. 2021;110(5):1317-1324. doi:10.1016/j.ijrobp.2021.03.031
20. Chaudary N, Pintilie M, Hedley D, Hill RP, Milosevic M, Mackay H. Hedgehog inhibition enhances efficacy of radiation and cisplatin in orthotopic cervical cancer xenografts. *Br J Cancer*. 2017;116(1):50-57. doi:10.1038/bjc.2016.383
21. Chaudary N, Pintilie M, Jelveh S, Lindsay P, Hill RP, Milosevic M. Plerixafor improves primary tumor response and reduces metastases in cervical cancer treated with radio-chemotherapy. *Clin Cancer Res*. 2017;23(5):1242-1249. doi:10.1158/1078-0432.Ccr-16-1730
22. Chaudary N, Pintilie M, Schwock J, et al. Characterization of the tumor microenvironment in patient-derived cervix xenografts (OCICx). *Cancers*. 2012;4(3):821-845. doi:10.3390/cancers4030821
23. Lecavalier-Barsoum M, Chaudary N, Han K, Pintilie M, Hill RP, Milosevic M. Targeting CXCL12/CXCR4 and myeloid cells to improve the therapeutic ratio in patient-derived cervical cancer models treated with radio-chemotherapy. *Br J Cancer*. 2019;121(3):249-256. doi:10.1038/s41416-019-0497-3
24. The Vancouver Prostate Centre and British Columbia Cancer Agency Research Centre. LTL-545 human prostate cancer xenograft. Accessed January 20, 2024. http://www.livingtumorlab.com/Data%20Sheets/2009-4-7-Prostate/LTL-545.pdf
25. Treuting PM, Dintzis SM. Male reproductive system. *Comparative Anatomy Histology: A Mouse and Human Atlas*. Elsevier; 2012.
26. Ittmann M. Anatomy and histology of the human and murine prostate. *Cold Spring Harbor Perspect Med*. 2018;8(5):a030346. doi:10.1101/cshperspect.a030346
27. Oliveira DSM, Dzinic S, Bonfil AI, Saliganan AD, Sheng S, Bonfil RD. The mouse prostate: a basic anatomical and histological guideline. *Bosn J Basic Med Sci*. 2016;16(1):8-13. doi:10.17305/bjbms.2016.917

28. Fagerland SMT, Hill DK, van Wamel A, de Lange Davies C, Kim J. Ultrasound and magnetic resonance imaging for group stratification and treatment monitoring in the transgenic adenocarcinoma of the mouse prostate model. *Prostate*. 2020;80(2):186-197. doi:10.1002/pros.23930
29. Bhandari V, Hoey C, Liu LY, et al. Molecular landmarks of tumor hypoxia across cancer types. *Nature Genet*. 2019;51(2):308-318. doi:10.1038/s41588-018-0318-2
30. Dhani N, Fyles A, Hedley D, Milosevic M. The clinical significance of hypoxia in human cancers. *Semin Nucl Med*. 2015;45(2):110-121. doi:10.1053/j.semnuclmed.2014.11.002
31. Guo H, Ci X, Ahmed M, et al. ONECUT2 is a driver of neuroendocrine prostate cancer. *Nat Commun*. 2019;10(1):278. doi:10.1038/s41467-018-08133-6
32. Lalonde E, Ishkanian AS, Sykes J, et al. Tumour genomic and microenvironmental heterogeneity for integrated prediction of 5-year biochemical recurrence of prostate cancer: a retrospective cohort study. *Lancet Oncol*. 2014;15(13):1521-1532. doi:10.1016/S1470-2045(14)71021-6
33. Milosevic M, Warde P, Ménard C, et al. Tumor hypoxia predicts biochemical failure following radiotherapy for clinically localized prostate cancer. *Clin Cancer Res*. 2012;18(7):2108-2114. doi:10.1158/1078-0432.CCR-11-2711
34. Ragnum HB, Vlatkovic L, Lie AK, et al. The tumour hypoxia marker pimonidazole reflects a transcriptional programme associated with aggressive prostate cancer. *Br J Cancer*. 2015;112(2):382-390. doi:10.1038/bjc.2014.604
35. Vergis R, Corbishley CM, Norman AR, et al. Intrinsic markers of tumour hypoxia and angiogenesis in localised prostate cancer and outcome of radical treatment: a retrospective analysis of two randomised radiotherapy trials and one surgical cohort study. *Lancet Oncol*. 2008;9(4):342-351. doi:10.1016/S1470-2045(08)70076-7

How to cite this article: Chaudary N, Wiljer E, Foltz W, Thapa P, Hill RP, Milosevic M. An orthotopic prostate cancer model for new treatment development using syngeneic or patient-derived tumors. *Prostate*. 2024;1-9. doi:10.1002/pros.24701